The Journal of Immunology
RESEARCH ARTICLE | SEPTEMBER 01 2017

Epithelial TNF Receptor Signaling Promotes Mucosal Repair in Inflammatory Bowel Disease FREE

Emily M. Bradford; ... et. al

J Immunol (2017) 199 (5): 1886–1897.
https://doi.org/10.4049/jimmunol.1601066

Epithelial TNF Receptor Signaling Promotes Mucosal Repair in Inflammatory Bowel Disease

Emily M. Bradford,*,†,[1] Stacy H. Ryu,*,‡,[1] Ajay Pal Singh,* Goo Lee,* Tatiana Goretsky,*,† Preetika Sinh,* David B. Williams,* Amber L. Cloud,† Elias Gounaris,* Vihang Patel,† Olivia F. Lamping,† Evan B. Lynch,† Mary Pat Moyer,§ Isabelle G. De Plaen,¶ David J. Shealy,‖ Guang-Yu Yang,# and Terrence A. Barrett*,†

TNF plays an integral role in inflammatory bowel disease (IBD), as evidenced by the dramatic therapeutic responses in Crohn's disease (CD) patients induced by chimeric anti-TNF mAbs. However, treatment of CD patients with etanercept, a decoy receptor that binds soluble TNF, fails to improve disease. To explore this discrepancy, we investigated the role of TNF signaling in Wnt/β-catenin–mediated intestinal stem cell and progenitor cell expansion in CD patients, human cells, and preclinical mouse models. We hypothesized that TNF exerts beneficial effects on intestinal epithelial cell (IEC) responses to injury. In CD patients, intestinal stem cell and progenitor cell Wnt/β-catenin signaling correlates with inflammation status. TNF-deficient ($Tnf^{-/-}$) mice exhibited increased apoptosis, less IEC proliferation, and less Wnt signaling when stimulated with anti-CD3 mAb. Bone marrow (BM) chimera mice revealed that mucosal repair depended on TNF production by BM–derived cells and TNFR expression by radioresistant IECs. Wild-type→$Tnfr1/2^{-/-}$ BM chimera mice with chronic dextran sodium sulfate colitis exhibited delayed ulcer healing, more mucosal inflammation, and impaired Wnt/β-catenin signaling, consistent with the hypothesis that epithelial TNFR signaling participates in mucosal healing. The direct effect of TNF on stem cells was demonstrated by studies of TNF-induced Wnt/β-catenin target gene expression in murine enteroids and colonoid cultures and TNF-induced β-catenin activation in nontransformed human NCM460 cells (TOPFlash) and mice (TOP-GAL). Together, these data support the hypothesis that TNF plays a beneficial role in enhancing Wnt/β-catenin signaling during ulcer healing in IBD. These novel findings will inform clinicians and therapeutic chemists alike as they strive to develop novel therapies for IBD patients. ***The Journal of Immunology*****, 2017, 199: 1886–1897.**

Tumor necrosis factor is a central regulator of inflammation and has been implicated in human diseases, including psoriasis, ankylosing spondylitis, rheumatoid arthritis, and inflammatory bowel diseases (IBDs) (1). TNF interacts with TNFR1 and TNFR2, which are differentially expressed on intestinal bone marrow (BM)-derived cells (macrophages/monocytes, lymphocytes, NK cells, and dendritic cells), as well as stromal cells (myofibroblasts, mesenchymal cells), and intestinal epithelial cells (IECs). In Crohn's disease (CD) and ulcerative colitis, diarrhea, mucosal ulceration, and intestinal bleeding are associated with high tissue levels of TNF along with the cytokines IFN-γ, IL-17, and IL-12 (2–5); however, the direct effects of these inflammatory molecules on epithelial cells remain uncertain.

Most biologic therapies targeting TNF have been successful at rapidly controlling inflammation in the majority of IBD patients; however, clinical data show that etanercept, a decoy receptor that binds to soluble TNF, is either ineffective or detrimental in the treatment of CD (6). Anti-TNF mAbs, such as infliximab and adalimumab, dampen inflammation by inducing apoptosis in immune cells (i.e., monocytes) expressing membrane-bound TNF through reverse signaling (7). In contrast, etanercept reduces levels of soluble TNF without directly binding mucosal leukocytes. We postulate that the deleterious effects of etanercept may be due to neutralization of TNF, which is needed for the epithelial response in colitis.

Examination of tissues from IBD patients reveals that inflammation affects epithelial proliferation, death, and lineage com-

*Department of Internal Medicine, Ann & Robert H. Lurie Children's Hospital of Chicago, Northwestern University Feinberg School of Medicine, Chicago, IL 60611; †Division of Gastroenterology, University of Kentucky, Lexington, KY 40536; ‡Driskill Graduate Program in Life Sciences, Ann & Robert H. Lurie Children's Hospital of Chicago, Northwestern University Feinberg School of Medicine, Chicago, IL 60611; §INCELL Corporation, San Antonio, TX 78249; ¶Department of Pediatrics, Ann & Robert H. Lurie Children's Hospital of Chicago, Northwestern University Feinberg School of Medicine, Chicago, IL 60611; ‖Janssen Research & Development, Radnor, PA 19087; and #Department of Pathology, Ann & Robert H. Lurie Children's Hospital of Chicago, Northwestern University Feinberg School of Medicine, Chicago, IL 60611

[1]E.M.B. and S.H.R. contributed equally to this work.

ORCIDs: 0000-0002-5448-339X (S.H.R.); 0000-0003-3025-5234 (G.L.); 0000-0001-8679-9711 (E.G.); 0000-0002-0297-8921 (M.P.M.); 0000-0002-9591-976X (D.J.S.).

Received for publication July 13, 2016. Accepted for publication June 27, 2017.

This work was supported by a Veterans Affairs Merit Award (I01CX001353-0141 to T.A.B.), the National Institutes of Health (Grants R01AI061701 and R01DK-095662 to T.A.B.), the Training Program in Oncogenesis and Developmental Biology through the National Cancer Institute (T32 CA080621, to support E.M.B.), and an Institutional Development Award from the National Institute of General Medical Sciences, National Institutes of Health (8 P20GM103527-05, to support tissue processing). Imaging work was also performed at the Northwestern Cell Imaging Facility, supported by National Cancer Institute Cancer Center Support Grant P30 CA060553 awarded to the Robert H. Lurie Comprehensive Cancer Center.

Address correspondence and reprint requests to Dr. Emily M. Bradford, Division of Gastroenterology, University of Kentucky, 800 Rose Street, MN 649, Lexington, KY 40536. E-mail address: emily.bradford@uky.edu

The online version of this article contains supplemental material.

Abbreviations used in this article: BM, bone marrow; BMC, BM chimera; CBC, crypt base columnar cell; CD, Crohn's disease; DSS, dextran sodium sulfate; IBD, inflammatory bowel disease; IEC, intestinal epithelial cell; ISC, intestinal stem cell; PC, progenitor cell; p–β-catenin^{552}, phosphorylation of β-catenin at Ser^{552}; WT, wild-type.

mitment. Chronic inflammation associated with IBD leads to architectural distortion that is characterized by crypt branching and fissioning (glandular irregularity), as well as goblet cell depletion. Alterations in crypt structure and composition seen in IBD suggest that mucosal inflammation affects signaling events in intestinal stem cell (ISC) and progenitor cell (PC) populations (8). During acute ulceration, the intestinal epithelium develops hyperproliferative crypts at ulcer margins by activating ISC/PC populations (9). These proliferative cells then support migration across ulcer surfaces, re-epithelialization, and the subsequent establishment of new crypt structures.

Maintenance of ISC and PC proliferative zones requires active Wnt/β-catenin signaling (10). Noggin and epidermal growth factor cooperate with β-catenin signaling, because the addition of these factors expands primary epithelial stem cells (11). Data from our group (12) and other investigators (13) show that PI3K signaling cooperates with Wnt to regulate stem cell behavior in the intestine. Models of mutated *BMPR1A* (14) and deficient *PTEN* (13) signaling indicate that Akt activation enhances β-catenin signaling. Increased PI3K activation leads to Akt phosphorylation of β-catenin at Ser^{552} (p–β-$catenin^{552}$) (13). We implicated this mechanism in mucosal inflammation by showing that T cell activation, as well as colitis, in $IL10^{-/-}$ mice increases nuclear p–β-$catenin^{552}$ in small bowel and colonic ISCs (12). These findings are consistent with the idea that inflammatory mediators released in the local environment activate relevant signaling pathways that enhance Wnt/β-catenin signaling.

Based on data from colitis patients and mouse models, we hypothesized that TNF supports Wnt/β-catenin signaling at times of severe inflammation and in ulceration. This was tested in wild-type (WT) and $Tnf^{-/-}$ mice. Although tissue histology and Wnt/β-catenin signaling were unperturbed in untreated $Tnf^{-/-}$ mice, T cell activation with anti-CD3 mAb (anti–T cell coreceptor mAb) induced widespread crypt distortion owing to a failure of Wnt/β-catenin signaling and proliferation in ISC/crypt base columnar cell (CBC) and transit-amplifying populations. The idea that TNF from BM-derived cells acts directly on epithelial cells was supported by data in BM chimera (BMC) mice and in vitro enteroid and colonoid models. BMC mice lacking epithelial TNFR1/2 revealed that epithelial TNFR signaling is beneficial during ulcer healing in chronic dextran sodium sulfate (DSS) colitis. These data identify TNF as a critical mediator of epithelial responses to severe mucosal inflammation with implications in stem cell activation.

Materials and Methods

Animal studies

C57BL/6 (WT), $Tnf^{-/-}$, $TNFR1/2^{-/-}$, BAT-GAL, and TOP-GAL mice were purchased from The Jackson Laboratory (Bar Harbor, ME). All mice were used at 8–14 wk of age and were housed in the Northwestern University or University of Kentucky animal care facilities under specific pathogen–free conditions. For T cell activation, anti-CD3 mAb (145-2C11; 10 mg/kg) or control hamster mAb (UC8-IB9) was administered at 15 mg/kg i.p. Mice were injected i.p. with 0.1 mg of BrdU (Sigma, St. Louis, MO) 2 h before sacrifice. For anti-TNF studies, mice were injected i.p. with 50 mg/kg rat/mouse chimeric monoclonal IgG2a,κ Ab specific for mouse TNF (CNTO 2213 lot number 0707-05V, a gift from D. Shealy, Johnson & Johnson Pharmaceuticals, New Brunswick, NJ). For the untreated group, CNTO 1322 lot number 0218-03T, a rat/mouse chimeric monoclonal IgG2a,κ negative-control Ab, was injected i.p. For in vivo TNF injection, PBS or recombinant murine TNF (100 μg/kg; PeproTech) was injected i.p. For BMC studies, recipient mice were irradiated with 9.5 Gy. BM was harvested from donor femurs, RBCs were lysed, and cells were filtered and counted on a hemocytometer. Recipient mice received five million donor cells by retro-orbital injection and were provided antibiotics for 14 d. Mice were given 8 wk to allow for stable engraftment prior to experimentation. To induce chronic colitis, mice were provided 2.5% DSS in the drinking water ad libitum for 7 d, followed by 14 d of water. This was repeated for three cycles, and mice were euthanized 6 d following the last cycle of DSS. All studies and procedures were approved by the Animal Care and Use Committees of Northwestern University and the University of Kentucky.

NCM TOPFlash assay

NCM460 cells (normal-derived colon mucosa) were received through a cell-licensing agreement with INCELL and were routinely propagated under standard conditions in M3:10 medium with the addition of conditional medium (30%) from previously cultured NCM460 cells. Cells were transfected with a reporter construct containing TCF/luc to evaluate β-catenin transcription. Transfected cells were treated overnight with 1 ng/ml TNF. Luciferase was detected with Luciferase reagent (Promega, Madison, WI).

Histological analysis

Ten-centimeter segments of ileum or colon were fixed in formalin, embedded in paraffin, and sectioned at 5 μm. The following Abs were used: anti-BrdU (MBL, Woburn, MA), anti-Ki67 clones TEC-3 and MIB-1 (Dako, Carpinteria, CA), anti–c-Myc (N-262; Santa Cruz Biotechnology, Dallas, TX), anti-survivin (NB500-201; Novus Biologicals, Littleton, CO), and anti-cleaved caspase-3 (Cell Signaling Technology, Danvers, MA). For TUNEL staining, an In Situ Cell Death Detection Kit, POD (Roche, Basel, Switzerland) was used. For BAT-GAL and TOP-GAL mice, β-galactosidase staining was performed, as described (15), and the number of $\beta\text{-galactosidase}^{+}$ cells per well-oriented crypt was counted in a minimum of eight sections. For colitis assessment, blinded evaluation was performed independently by two investigators (G.L. and G.-Y.Y.). Colitis in human biopsy specimens was scored from 0 to 4 based on the increasing severity of mononuclear infiltration and epithelial ulceration, with immunohistochemical analysis performed on chronically inflamed adjacent mucosa.

Real-time semiquantitative RT-PCR

Total RNA was isolated from 0.5-cm segments of the intestine or cultured cells using an RNeasy Mini Kit (QIAGEN, Valencia, CA) and reverse transcribed using a High-Capacity cDNA Reverse Transcription Kit (Applied Biosystems, Foster City, CA). Real-time PCR used an AB StepOnePlus Real-Time PCR system and Power SYBR Green PCR Master Mix (both from Applied Biosystems). Primers were designed by Primer Express software 3.0 (Applied Biosystems) based on nucleotide sequences from the National Center for Biotechnology Information data bank. For each sample, the threshold value for *Gapdh* was determined and used as an internal reference. All assays were performed in triplicate, and fold changes were calculated using the ΔΔ cycle threshold method.

Enteroid/colonoid culture

Small intestine and colonic crypts were isolated and cultured in a three-dimensional system, as described previously (11, 16). Crypts were embedded in Matrigel (BD Biosciences) and seeded in a prewarmed 24-well plate at ~200 crypts in 50 μl. After the Matrigel solidified, 500 μl of 50% L-WRN media was overlaid (16).

Cytokine stimulation of enteroid/colonoid culture

Enteroids and colonoids were propagated for 1 wk, passaged, and cultured for 24 h in 50% L-WRN media, and media were changed to 25% L-WRN containing 0, 1, or 10 ng/ml rTNF (PeproTech). TNF concentrations were based on experiments (above) showing that 1 ng/ml is sufficient to induce TOPFlash reporter activation in NCM cells. Cells were cultured for five additional days and measured for size (diameter) and budding every other day. For RNA analysis, the Matrigel was washed with PBS, and enteroids/colonoids were lysed directly in Buffer RLT (QIAGEN). RNA was isolated using an RNeasy Mini Kit (QIAGEN).

Human colonic specimens

Human colonic biopsy specimens were obtained from patients undergoing diagnostic or surveillance colonoscopy for known or suspected CD who were receiving anti-TNF mAb alone or no therapy (untreated) and were collected at Northwestern University or at the University of Kentucky. All untreated patients with active CD and those that had active disease that was refractory to anti-TNF had moderate to severe active CD (CD Activity Index ≥ 200). The CD Activity Index was not significantly different between untreated CD patients and anti-TNF–treated patients. For comparison, biopsy specimens were obtained from healthy patients undergoing routine colon cancer surveillance, as well as from patients with CD currently in remission and on anti-TNF therapies. Collection of all patient materials for this study was approved by Northwestern University's Office for the Protection of Human Subjects or the University of Kentucky Institutional Review Board.

Western blot analysis

Human and mouse tissues were homogenized in Buffer I (50 mM Tris-HCl, 100 mM NaCl, 0.01% digitonin), disrupted with a 26G needle, and centrifuged at 4˚C at maximum speed. The supernatant was taken as the cytosolic fraction. The pellets were resuspended in Buffer II (50 mM Tris-HCl, 2% Triton X-100, 100 mM NaCl), incubated on ice for 30 min, and centrifuged as above. The supernatant was taken as the membrane/organelle fraction. To obtain nuclear fractions, the remaining pellet was dissolved in Buffer III (50 mM Tris-HCl, 0.25% n-dodecyl-D-maltoside, 100 mM NaCl, and 20 U/ml Benzonase [Sigma]), incubated for 30 min at room temperature, and centrifuged. The pellet was discarded. Proteins were subjected to SDS-PAGE and transferred to Immobilon-FL membranes (Millipore, Billerica, MA). Membranes were probed for actin (Sigma), axin2 (Abcam, Cambridge, U.K.), p–β-catenin^{552} (gift of L. Li, Stowers Institute for Medical Research), BMP4 (Abcam), c-Myc (Cell Signaling Technology), cyclin D1 (Santa Cruz Biotechnology), and lamin B1 (Zymed; Thermo Fisher, Waltham, MA).

Statistical analysis

Statistical analyses were performed using Prism software (GraphPad). For more than two groups, data were compared by one-way ANOVA, followed by a post hoc Tukey test. For comparison of two groups, the Student *t* test was used. The p values ≤ 0.05 were considered statistically significant. Unless specified, data represent mean ± SEM (17).

Results

TNF mediates epithelial β-catenin signaling and proliferation in CD patients

To examine whether TNF signaling affects Wnt/β-catenin signaling during mucosal inflammation, we examined the levels of epithelial nuclear p–β-catenin^{552} and cyclin D1 in colonic biopsy samples of healthy untreated patients ($n = 7$), active untreated CD patients ($n = 8$), and anti-TNF mAb–treated CD patients who were refractory to treatment ($n = 9$) or were in remission ($n = 10$). Both subsets of clinically active CD patients had active tissue inflammation based on histological analysis (Fig. 1A). As expected, inflammatory scores correlated with epithelial proliferation, as examined by Ki67 staining (Fig. 1B). The number of Ki67^{+} cells per crypt was elevated in inflamed tissues (healthy 18 ± 7, active untreated CD 39 ± 7.1, and active anti-TNF–treated CD 33 ± 3) and reduced in patients on anti-TNF mAb treatment who were in remission (23 ± 3).

TNF mediates epithelial β-catenin signaling in human and mouse IECs

To examine whether TNF directly promotes Wnt/β-catenin signaling in human cells, NCM460-nontransformed human colonic epithelial cells were transfected with the TOPFlash construct, which reports TCF/LEF transcriptional activation. TNF treatment increased β-catenin/TCF luciferase reporter activity, consistent with enhanced transcriptional activation of this promoter (Fig. 2A). These findings were supported by Western blot data in NCM460 cells in which TNF significantly increased cyclin D1 and c-Myc, both products of β-catenin target gene expression (Fig. 2B). Based on these data, we speculate that TNF induces epithelial Wnt/β-catenin activation and proliferation during mucosal inflammation.

To determine whether TNF can induce β-catenin signaling in vivo, TOP-GAL mice, which report LEF1/TCF signaling and activated β-catenin through expression of *lacZ* were used. Mice were injected with rTNF, and cell positions were analyzed. As a control, one cohort of mice was treated with anti-TNF mAb 3 h prior to TNF injection. Untreated mice had β-galactosidase restricted to the crypt base in the small intestine and colon (Fig. 2C). Treatment with TNF increased the number of cells with active β-catenin signaling in the small intestine (1.5 ± 0.2 and 3.7 ± 0.6, untreated and TNF treated, respectively, $p < 0.05$) and colon (2.5 ± 0.9 and 9.5 ± 0.9, untreated and TNF treated, respectively, $p < 0.05$). Pretreatment with anti-TNF abolished this response (Fig. 2D).

TNF induces ISC gene expression downstream of β-catenin

Wnt/β-catenin signaling plays a crucial role in maintaining intestinal stem cells and PCs (18). Therefore, we next examined the role of TNF in Wnt/β-catenin signaling in ISCs and PCs using primary small intestinal enteroid (Fig. 3A) and colonoid (Fig. 3B) cultures. Data indicate that 5 d of TNF treatment induced several Wnt target genes in enteroids. Importantly, TNF significantly upregulated the expression of Ascl2, a Wnt target gene and key ISC transcription factor (19), in a dose-dependent manner (Fig. 3A). TNF also upregulated the Ascl2 target gene Ets2 (20) and Wnt-target CD44, both of which are implicated in stem cell maintenance and suppression of differentiation. TNF treatment did

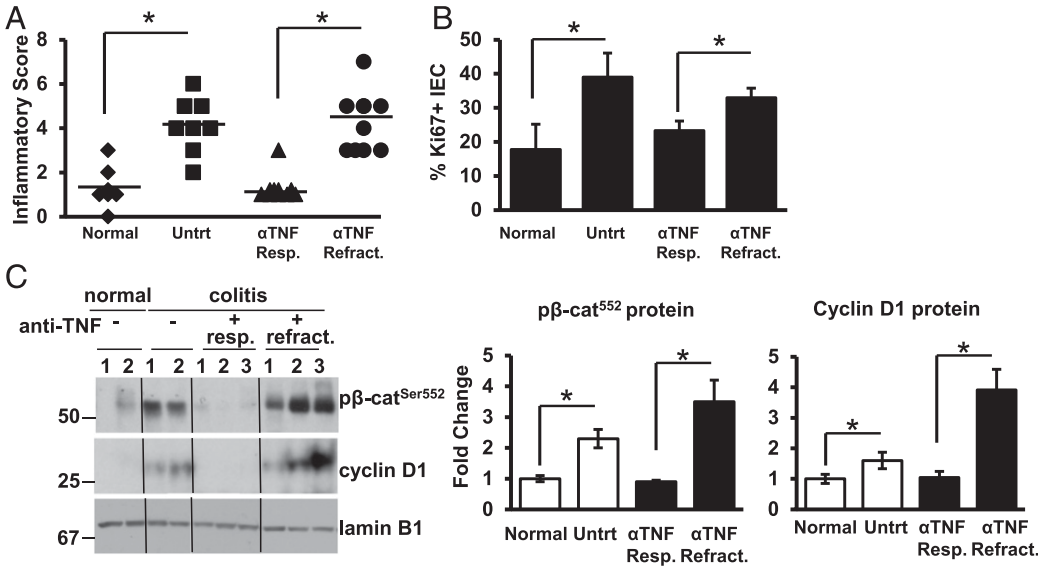

FIGURE 1. TNF mediates epithelial β-catenin signaling and proliferation. (**A**) Histological inflammatory scores for normal (healthy; $n = 7$), untreated CD ($n = 8$), anti-TNF–responsive ($n = 10$), and anti-TNF–refractory CD ($n = 10$) patients. Horizontal lines denote the average score of each group. (**B**) Ki67-stained cells per 100 IECs in normal, untreated CD, anti-TNF–responsive, and anti-TNF–refractory CD patients. (**C**) Immunoblot analysis and densitometry of p–β-catenin^{552} and cyclin D1 in nuclear fractions of isolated human colonic epithelial cells ($n = 2$ or 3 for each group). Data represent mean ± SEM, $^{*}p < 0.05$.

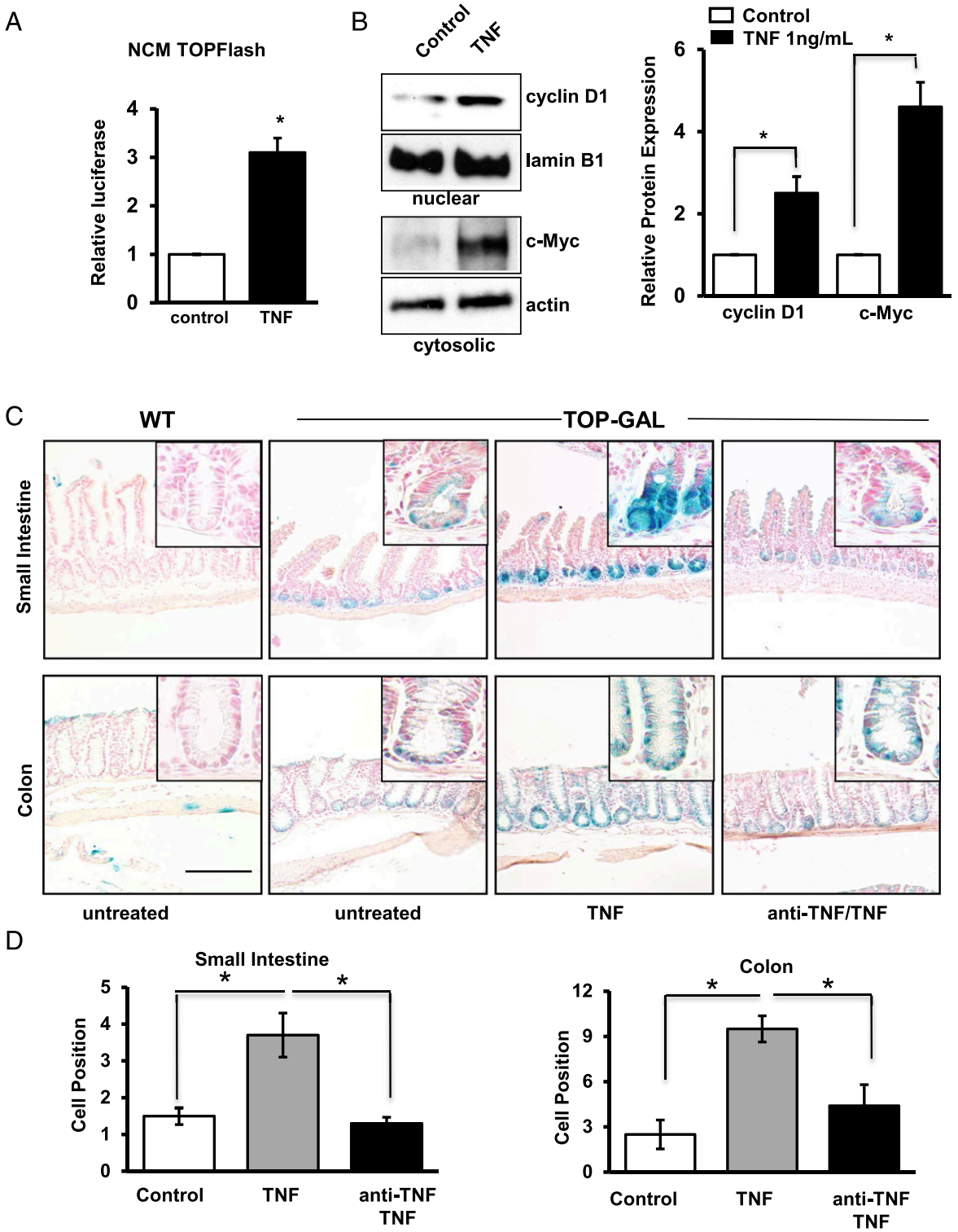

FIGURE 2. TNF and inflammation activate epithelial Wnt signaling. (**A**) TCF/LEF promoter activity measured as mean relative luciferase units in control and TNF-treated human nontransformed colonic NCM460 cells. (**B**) Western blot and corresponding densitometries of cytoplasmic and nuclear levels of cyclinD1 and c-Myc normalized to lamin B1 and actin, respectively, in control and TNF-treated NCM cells. Independent cell culture experiments were repeated four times (three to six wells of each treatment per experiment). (**C**) β-Galactosidase staining of control and TNF-treated (24 h) TOP-GAL mice, with and without anti-TNF treatment. Scale bar, 100 μm. (**D**) Quantification of the highest cell position with $LacZ^+$ staining in ileum and colon. A minimum of 20 well-oriented crypts were counted per mouse; $n = 3$ control mice, $n = 4$ mice treated with TNF, and $n = 4$ mice treated with anti-TNF and TNF. Data represent mean ± SEM. $*p < 0.05$.

not alter the mRNA expression of differentiation markers (AP, Muc2, TFF3, Lys, CK20) or markers of proliferation (Ki67 and PCNA). TNF did not alter the size of the enteroids (Fig. 3A), the percentage of enteroids that budded, or the number of buds per enteroid (Supplemental Fig. 1A). In colonoids, the stem cell markers Lgr5, Ascl2, Lrig (21), and Axin2 were upregulated by TNF, as was the β-catenin target gene CD44 (Fig. 3B). Markers of differentiation and proliferation were not significantly changed,

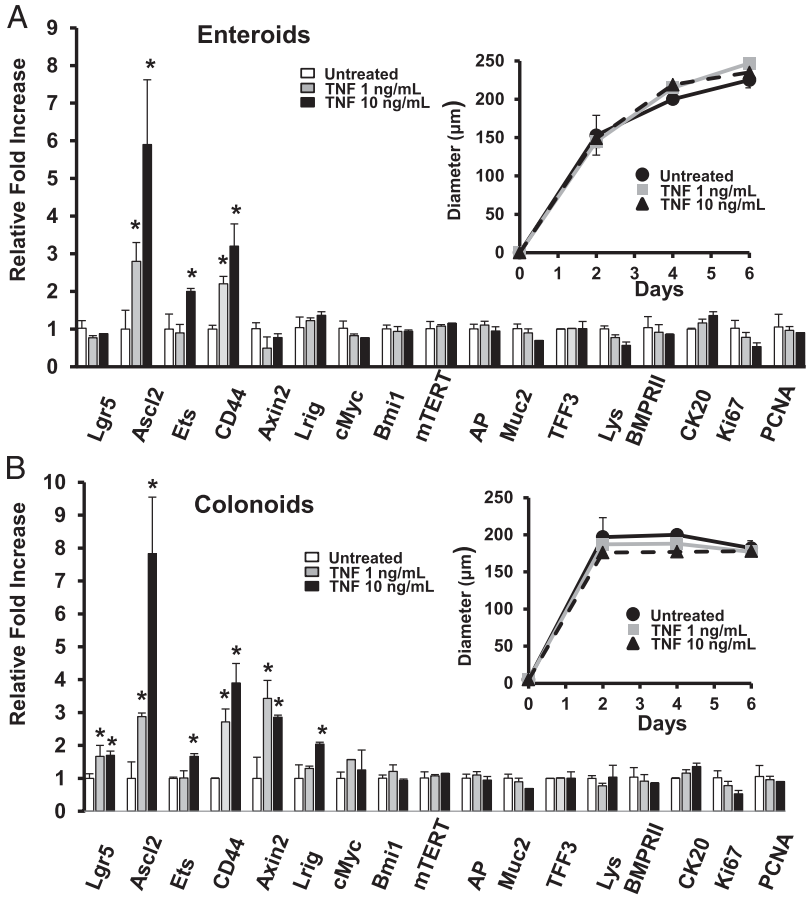

FIGURE 3. TNF promotes ISC activation. mRNA expression levels of stem cell markers and Wnt target genes (Lgr5, Ascl2, Ets, CD44, Axin2, Lrig, c-Myc, and mTERT), differentiation markers (AP, Muc2, TFF3, Lys, and CK20), and proliferation markers (Ki67 and PCMA) in mouse small intestinal enteroids (**A**) and mouse colonoids (**B**) cultured in the presence or absence of rTNF for 5 d. The diameters of enteroids and colonoids are shown as insets. Enteroids and colonoids were cultured in individual experiments from five separate mice. For each experiment, three to six wells were treated for each condition. Data represent mean ± SEM. *$p < 0.01$.

nor were the size (Fig. 3B) or budding characteristics of the colonoids (Supplemental Fig. 1B). Acute TNF treatment (4 and 24 h) did not induce any significant changes in Wnt target genes (data not shown). Taken together, these data suggest that TNF cooperates with Wnt signaling to enhance Wnt target gene expression needed for maintenance of intestinal ISC populations.

Loss of TNF impairs Wnt signaling, ISC activation, and IEC expansion during T cell activation

We next examined whether TNF signaling is required to induce mitogenic Wnt/β-catenin signaling during T cell activation. WT and *Tnf*$^{-/-}$ mice were treated with T cell–activating anti-CD3 mAb, and IEC responses were examined. Histology in WT mice revealed that T cell activation induced crypt elongation and mild villus blunting, as previously reported (22, 23). In contrast, T cell activation in *Tnf*$^{-/-}$ mice induced profound crypt dilation and exaggerated villus blunting, which was most pronounced 24 h following anti-CD3 treatment (Fig. 4A). Thus, data suggest that TNF mediates physiologic IEC responses to T cell activation.

Given the rapid crypt disruption and villus blunting in T cell–stimulated *Tnf*$^{-/-}$ mice, BrdU labeling was examined in WT and *Tnf*$^{-/-}$ mice (Fig. 4A, 4B). T cell activation increased BrdU labeling by 55% in WT IECs (control and anti-CD3–treated mice, 8.9 ± 0.7 and 14.3 ± 0.9 positive cells per crypt, respectively) (Fig. 4B). By comparison, IEC proliferative responses decreased by >80% in anti-CD3–treated *Tnf*$^{-/-}$ mice compared with unstimulated controls (control and anti-CD3–treated mice, 8.1 ± 0.6 and 1.3 ± 0.3 positive cells per crypt, respectively). These data suggest that TNF is required to sustain T cell–mediated proliferative responses in intestinal crypts.

In addition to proliferative responses, anti-CD3 treatment has been shown to induce a biphasic wave of apoptosis, with acute apoptosis of villus tips occurring in the first 4 h, and IEC death in crypts peaking around 24 h (24, 25). At 24 h, cleaved caspase-3 staining revealed a significant increase in crypt apoptosis in WT mice treated with anti-CD3 (WT untreated and WT anti-CD3 treated, undetectable and 0.2 ± 0.1 positive cells, respectively, $p < 0.05$). The response to anti-CD3 was exacerbated in *Tnf*$^{-/-}$ mice, and the number of apoptotic cells per crypt increased by 7-fold (1.5 ± 0.3 positive cells) (Fig. 4A, 4B).

Survivin, a member of the inhibitor of apoptosis family, is a downstream target of the Wnt/β-catenin pathway and is often induced as an adaptive response to epithelial damage (26–28). Additionally, survivin identifies PC populations in the gut (29, 30). Survivin staining (Supplemental Fig. 3) revealed a significant increase in survivin^{+} cells in T cell–stimulated WT mice (WT untreated and WT anti-CD3 treated, 8 ± 2 and 15 ± 3 positive cells per crypt, respectively, $p < 0.05$). In contrast, *Tnf*$^{-/-}$ mice failed to respond (*Tnf*$^{-/-}$ untreated and *Tnf*$^{-/-}$ anti-CD3 treated, 6 ± 2 and 6 ± 3 positive cells per crypt, respectively, NS) (Fig. 4B), indicating that TNF promotes survivin expression in mucosal inflammation.

Real-time PCR analysis of tissue from WT and *Tnf*$^{-/-}$ small intestine confirmed that *Tnf*$^{-/-}$ mice exhibit a significant downregulation of mRNA encoding the stem cell markers Axin2, Lgr5, and Sox9 in response to T cell activation (Fig. 4C). Gene-expression levels of PC markers c-Myc and survivin were modestly upregulated by anti-CD3 treatment; however, TNF deficiency did not affect c-Myc expression and only slightly reduced survivin levels in response to anti-CD3. Interestingly, inducible NO synthase

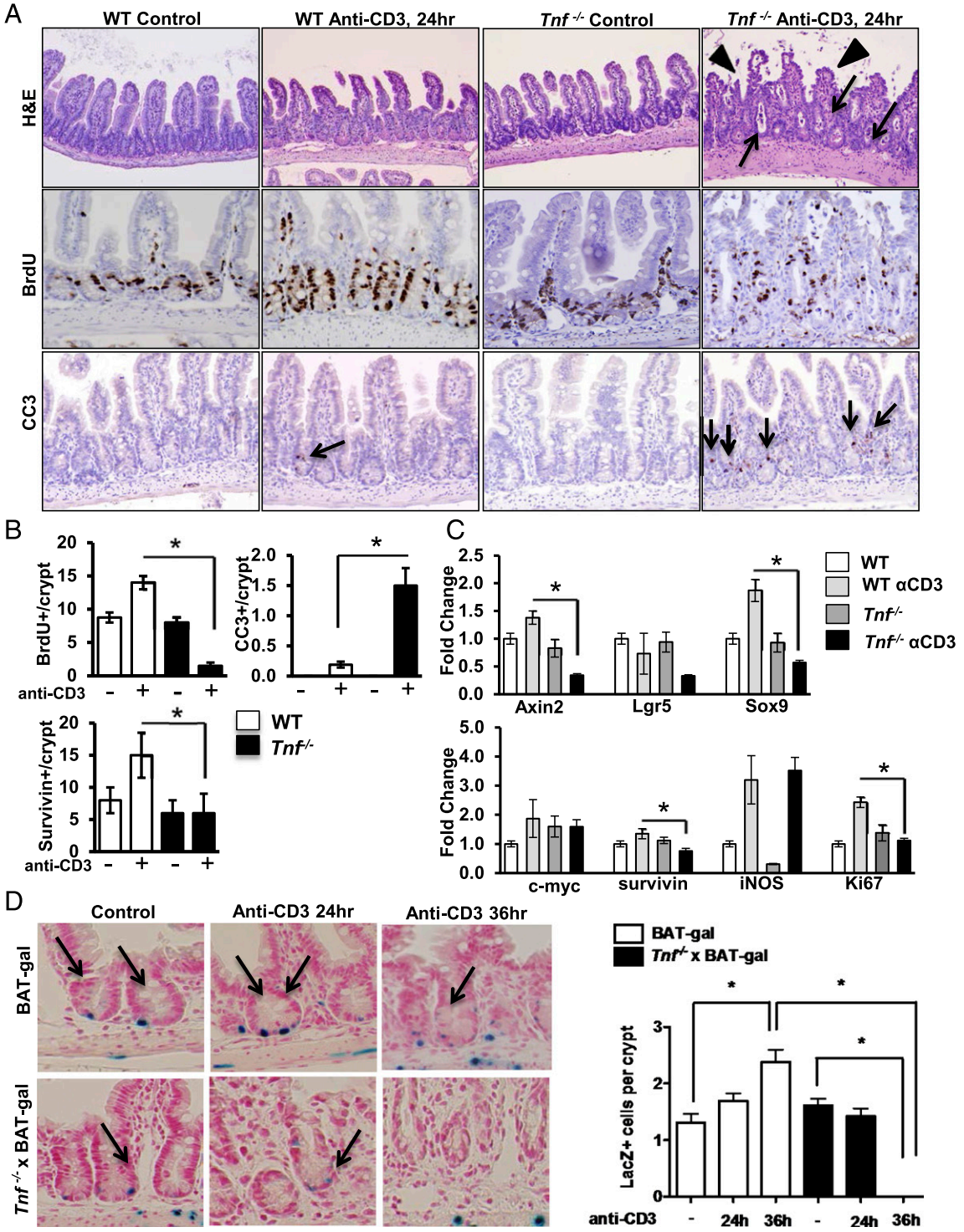

FIGURE 4. TNF mediates T cell–induced ISC and PC IEC activation in the small intestine. (**A**) Representative H&E staining of control and anti-CD3 mAb–treated WT and $Tnf^{-/-}$ mice at 24 h. Arrows denote crypt dilation with cellular debris, and arrowheads denote villus blunting (top panels). Representative images of BrdU and cleaved caspase-3 (CC3) staining. Survivin staining is shown in Supplemental Fig. 3. Arrows denote apoptotic cells (bottom panels). H&E images are shown at original magnification ×10 and BrdU and CC3 are shown original magnification ×20. (**B**) Numbers of $BrdU^+$, $CC3^+$, and $survivin^+$ cells detected per crypt. Positive cells were counted in ≥20 well-oriented crypt/villus axes per section. Data represent mean ± SEM. (**C**) mRNA expression levels of stem cell markers (Axin2, Lgr5, Sox9), progenitor cell markers (c-Myc, survivin), Ki67, and inducible NO synthase in ileum of WT and $Tnf^{-/-}$ mice. Anti-CD3 experiments in $Tnf^{-/-}$ mice were repeated twice; $n = 6$–8 mice per group. (**D**) β-Galactosidase staining of control and anti-CD3 mAb–treated BAT-GAL and $Tnf^{-/-}$ × BAT-GAL mice and quantification of nuclear β-galactosidase$^+$ IECs per well-oriented crypt. Positive cells were counted in ≥20 well-oriented crypts per section; $n = 3$ mice per group. Images are shown at original magnification ×40. Arrows identify nuclear β-galactosidase. Data represent mean ± SEM. $^*p < 0.05$.

was induced equally by anti-CD3 in WT and $Tnf^{-/-}$ mice. T cell–induced Ki67 mRNA induction was abrogated in $Tnf^{-/-}$ mice (Fig. 4C).

We analyzed WT and $Tnf^{-/-}$ mice 24 h following anti-CD3 treatment, based on previous reports and our own studies demonstrating profound differences in proliferation and crypt

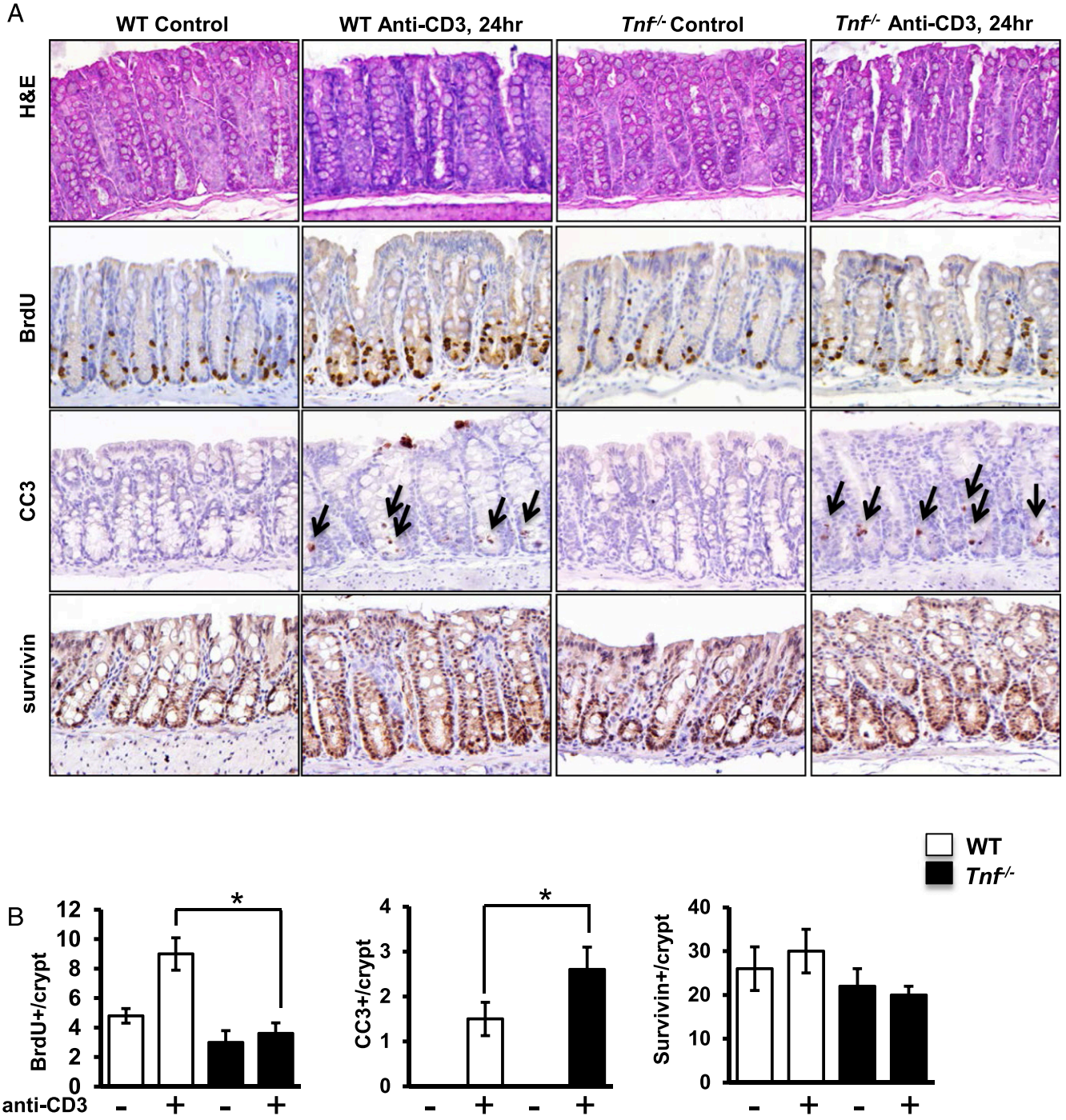

FIGURE 5. TNF mediates T cell–induced IEC activation in the colon. (**A**) Representative images of H&E, BrdU, cleaved caspase-3 (CC3), and survivin staining of control and anti-CD3 mAb–treated WT and $Tnf^{-/-}$ colon at 24 h. Images were taken at original magnification ×20. Arrows identify apoptotic cells. (**B**) Quantification of $BrdU^+$, $CC3^+$, and $survivin^+$ IECs detected per crypt. Positive cells were counted in ≥20 well-oriented crypts per section; n = 6–8 mice per group. Data represent mean ± SEM. $*p < 0.05$.

apoptosis at that time point. However, differences in mucosal cytokine expression between WT and $Tnf^{-/-}$ mice were observed as early as 3 h following anti-CD3 treatment, even though tissues appeared histologically normal (Supplemental Fig. 2). The proinflammatory cytokines IL-2, IL-6, and IL-1β were significantly upregulated in treated $Tnf^{-/-}$ mice at 3 h. At 18–24 h posttreatment, $Tnf^{-/-}$ mice displayed severe villus blunting and architectural distortion (Supplemental Figs. 2, 4). Crypt apoptosis and impaired proliferation persisted to 36 h posttreatment (data not shown); however, $Tnf^{-/-}$ mice exhibited increased proliferation, with normalization seen at 96 h (Supplemental Fig. 2).To determine whether anti-CD3 treatment regulates β-catenin signaling in the stem cell niche, BAT-GAL mice were used. Like TOP-GAL mice, BAT-GAL mice express the *lacZ* gene under the control of β-catenin/T cell factor response elements and are considered a reliable readout of Wnt signaling in a variety of tissues (31). Given that β-galactosidase staining in BAT-GAL mice is an in vivo indicator of Wnt/β-catenin signaling, we examined BAT-GAL and $Tnf^{-/-}$ × BAT-GAL mice after T cell activation. T cell activation doubled the numbers

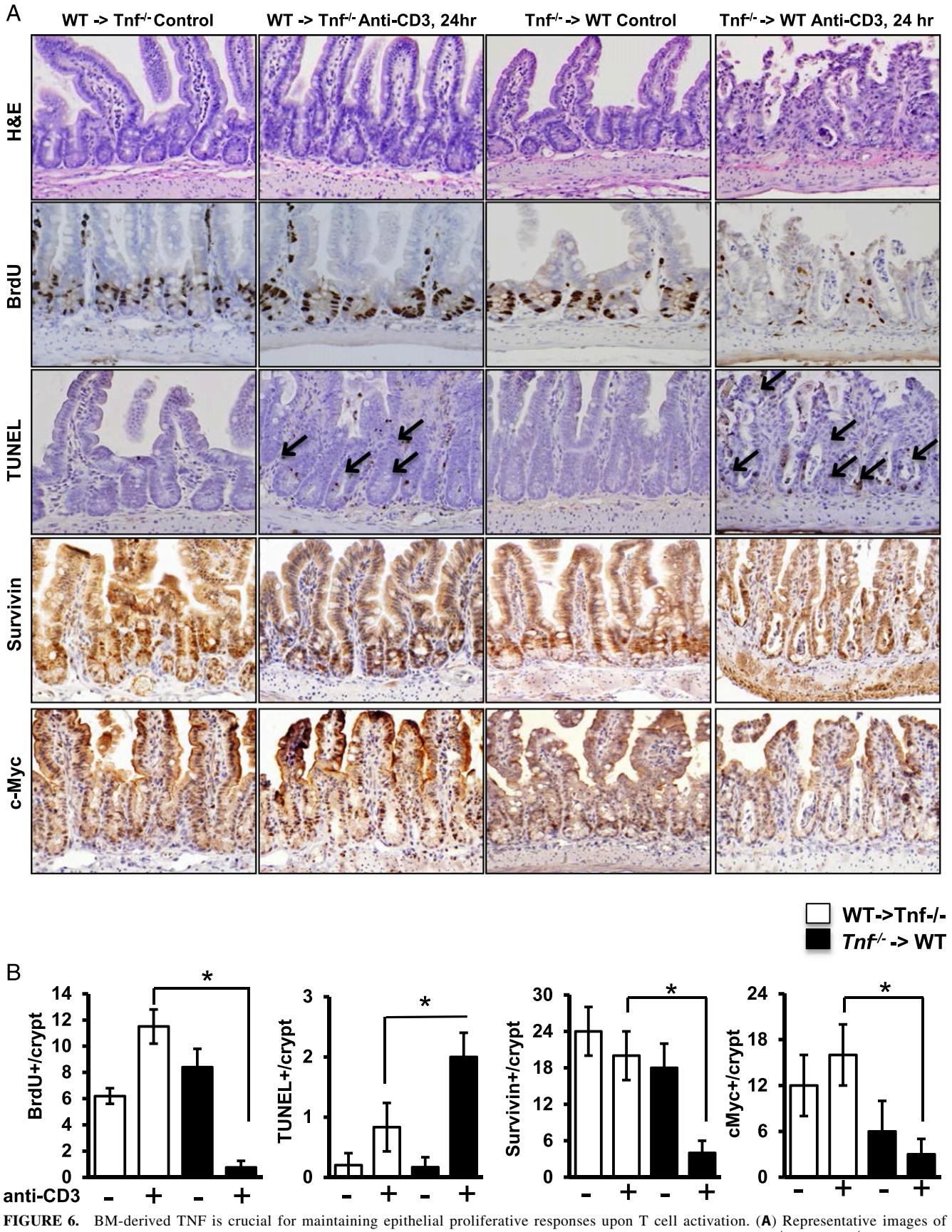

FIGURE 6. BM-derived TNF is crucial for maintaining epithelial proliferative responses upon T cell activation. (**A**) Representative images of H&E, BrdU, TUNEL, survivin, and c-Myc staining of ileal tissue from control- and anti-CD3–treated (24 h) WT→*Tnf*$^{-/-}$ and *Tnf*$^{-/-}$→WT BMC mice. Images were taken at original magnification ×20. Arrows indicate TUNEL^{+} IECs. (**B**) Quantification of BrdU^{+}, TUNEL^{+}, survivin^{+}, and c-myc^{+} cells per crypt. Positive cells were counted in ≥20 well-oriented crypt/villus axes per section; n = 6–8 mice per group. Data represent mean ± SEM. *$p < 0.05$.

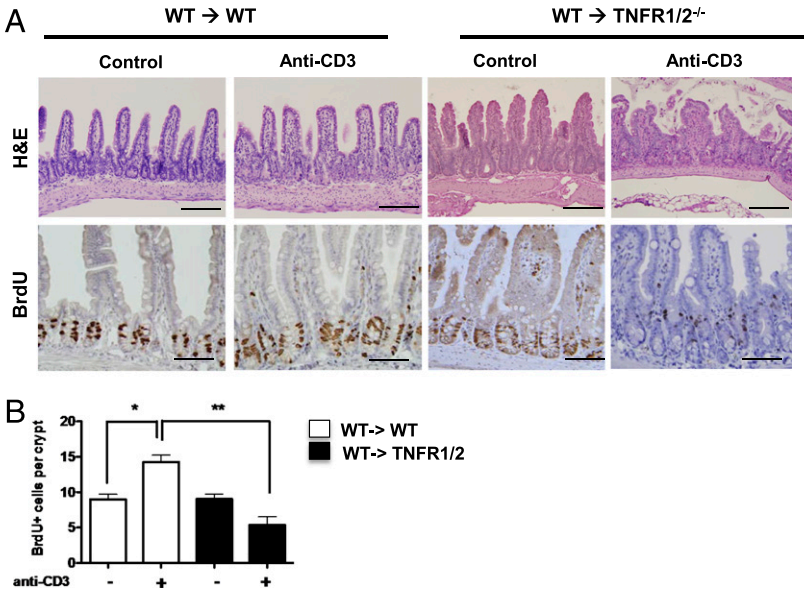

FIGURE 7. TNFR signaling mediates T cell–mediated IEC responses. (**A**) Representative images of H&E and BrdU staining for ileal tissue from control and anti-CD3–treated BMC mice. Scale bars, 150 μm. (**B**) Quantification of $BrdU^+$ cells per crypt. Positive cells were counted in ≥20 well-oriented crypt/villus axes per section; $n = 4$ mice per group. Data represent mean ± SEM. $*p < 0.01$, $**p < 0.001$.

of IECs with BAT-GAL expression, primarily in CBCs (high magnification in Fig. 4D, low magnification in Supplemental Fig. 2D). In comparison, BAT-GAL expression in CBCs was dramatically reduced in T cell–stimulated TNF-deficient mice. Similarly, examination of c-Myc, a Wnt/β-catenin target gene, revealed parallel responses upon T cell activation in WT and $Tnf^{-/-}$ mice (Supplemental Fig. 2C).

To determine whether TNF regulates IEC mitogenic responses in the colon, WT and $Tnf^{-/-}$ distal colon tissues were analyzed for proliferation and apoptosis at baseline and following T cell stimulation. Similar to the small intestine, T cell activation induced robust increases in proliferation (BrdU incorporation) in WT mice but not in $Tnf^{-/-}$ mice (Fig. 5). $Tnf^{-/-}$ mice also exhibited a 1.7-fold increase in the number of apoptotic cells per crypt in response to anti-CD3. In the colon, survivin was not significantly altered by anti-CD3 treatment in WT or $Tnf^{-/-}$ mice (Fig. 5).

BM-derived TNF and epithelial TNFRs are crucial for maintaining epithelial proliferative response upon T cell activation

To determine the source of TNF required for T cell–induced IEC responses, BMC mice were constructed using WT and $Tnf^{-/-}$ mice. T cell–induced epithelial responses (IEC BrdU incorporation and apoptosis) in WT→WT (donor→recipient, data not shown) and WT→$Tnf^{-/-}$ BMC mice closely resembled those detected in intact WT mice (Fig. 6, Supplemental Fig. 4). In comparison, IEC responses in $Tnf^{-/-}$→WT and $Tnf^{-/-}$→$Tnf^{-/-}$ BMC mice reflected changes seen in $Tnf^{-/-}$ mice. In particular, changes in BrdU staining in chimeric mice reconstituted with TNF-deficient BM closely mirrored IEC responses in intact $Tnf^{-/-}$ mice (Fig. 6). TUNEL staining demonstrated that $Tnf^{-/-}$→WT mice have a 2-fold increase in apoptotic cells (WT→$Tnf^{-/-}$ anti-CD3 and $Tnf^{-/-}$→WT anti-CD3, 0.9 ± 0.3 and 2.1 ± 0.3 cells, respectively, $p < 0.05$). Epithelial survivin and c-Myc staining were also abrogated in mice with TNF-deficient BM, suggesting impaired epithelial Wnt/β-catenin signaling in $Tnf^{-/-}$→WT mice (Fig. 6). These responses were recapitulated in colonic tissue of BMC mice (Supplemental Fig. 4). Together, the data suggest that TNF produced by BM-derived populations (e.g., macrophages, T cells, mast cells) mediates ISC and PC activation during mucosal immune responses.

Given the data indicating that TNF produced by BM-derived cells stimulates Wnt/β-catenin signaling in IECs, we next examined the requirements for TNFR expression in radiation-resistant epithelial cells in Wnt signaling. To determine the role of IEC TNFR expression in T cell–induced ISC and PC responses, BMC mice were generated with WT BM reconstitution of *Tnfrsf1a/b*$^{-/-}$ recipients (WT→*Tnfrsf1a/b*$^{-/-}$ [hereafter TNFR1/2$^{-/-}$]). Data show that T cell–induced architectural changes and BrdU incorporation (Fig. 7) in WT→WT BMC mice resembled those in intact WT mice. In contrast, increases in epithelial proliferation were abrogated in WT→TNFR1/2$^{-/-}$ BMC mice (data not shown). The results using BMC mice indicate that TNF production by BM-derived cells induces epithelial TNFR-mediated responses.

Epithelial TNFR signaling is crucial in promoting mucosal healing in chronic colitis

Given our findings that suggest that IEC TNFR signaling is critical for T cell–induced IEC responses in the colon, we examined the requirement for TNFR signaling in mediating colonic IEC responses to chronic colitis (Fig. 8). Following three cycles of 2.5% DSS, mice develop a highly reproducible course of colitis that is characterized by ulceration, inflammatory infiltrates, hyperplasia of epithelium, and crypt branching. In WT mice, severe ulceration (60–80% denuded epithelium) peaks 3 d after the withdrawal of DSS, and the mice recover completely in the following 11 d. Healing can be measured as the percentage of colonic surface with intact crypts (Fig. 8B); to observe both damaged and healing epithelium, mice are analyzed 6 d following withdrawal of DSS. Compared with WT→WT BMC mice, BMC mice with deficient TNFR1/2 expression (WT→TNFR1/2$^{-/-}$) exhibited a more severe response to colitis, as measured by increased total ulceration (Fig. 8C), reduced surface area with intact crypts (Fig. 8D), and an increased colitis score (Fig. 8E). β-catenin signaling was measured by Western blot analysis of epithelial protein isolates, demonstrating that the increased nuclear p–β-catenin^{552} and cytosolic AXIN2 seen in WT→WT mice with colitis were abrogated in WT→TNFR1/2$^{-/-}$ BMC mice (Fig. 8F). Interestingly, although healing was delayed in WT→TNFR1/2$^{-/-}$ BMC mice, complete re-epithelialization was completed by 14 d following DSS (relative to complete healing at 7 d in WT→WT mice, data not shown). It is possible that nonepithelial radio-resistant populations of cells (e.g.,

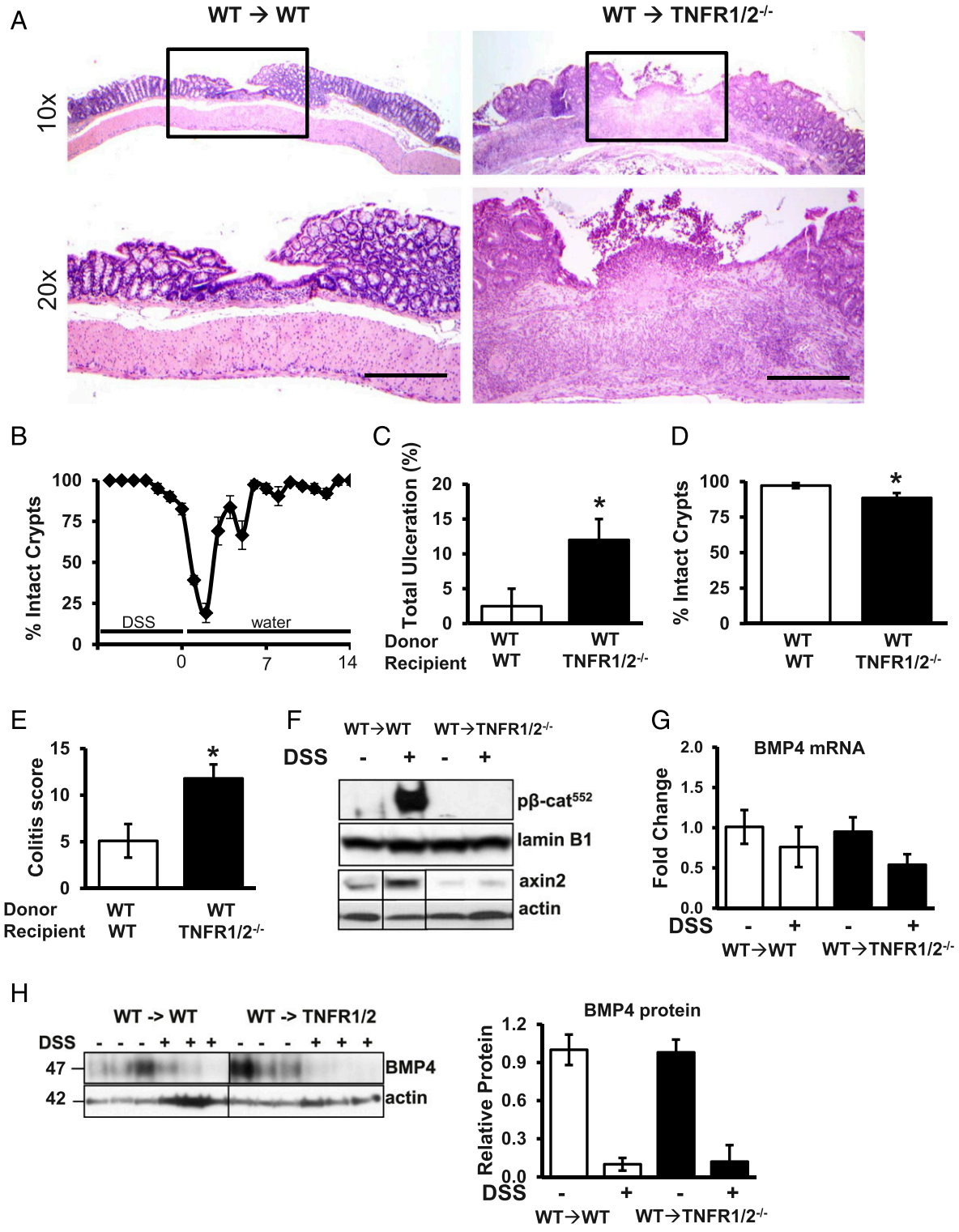

FIGURE 8. Epithelial TNFR signaling is required for mucosal healing after DSS treatment. (**A**) Representative histology of colons from WT→WT and WT→TNFR1/2$^{-/-}$ BMC mice 6 d following three cycles of 2.5% DSS. Scale bars, 1.5 mm. (**B**) Graphical representation of healing in WT mice treated with DSS (n = 3–6 mice at each time point). Percentage of colonic surface area containing intact crypts during and after the last cycle of DSS is shown. The percentage of ulcerated area (**C**) and percentage of area with intact crypts (**D**) 6 d following DSS withdrawal. (**E**) Colitis scores for WT→WT and WT→TNFR1/2$^{-/-}$ BMC mice treated with DSS. (**F**) Western blot of nuclear p–β-catenin^{552} and axin2 from isolated IECs from WT→WT and WT→TNFR1/2$^{-/-}$ colon. (**G** and **H**) mRNA and protein levels of BMP4 from colonic tissue isolated from WT→WT and WT→TNFR1/2$^{-/-}$ colon. n = 5 mice for each group. Data represent mean ± SEM. *$p < 0.05$.

tissue macrophages, fibroblasts) contribute to the healing response in this model. Although we cannot rule out this contribution, we analyzed tissue samples for mRNA expression (Fig. 8G) and protein levels (Fig. 8H) of BMP4. DSS treatment reduced BMP4 levels to the same degree in WT→WT and WT→TNFR1/2$^{-/-}$ mice. Together, these data suggest that epithelial TNFR signaling is crucial for promoting mucosal healing by mediating ISC/PC activation during chronic colitis.

Discussion

Canonical Wnt/β-catenin plays a crucial role in mucosal wound healing (32, 33). Stappenbeck and colleagues (34) presented strong evidence that noncanonical Wnt (e.g., Wnt5a) contributes to wound healing by allowing expanding crypts to form clefts at wound edges. The demonstration that noncanonical Wnt signaling opposes canonical signals (9) raises the attractive hypothesis that ulcer healing in IBD occurs as an outcome of factors that both promote and oppose Wnt signaling (35). Data presented in this article suggest that TNF may be a positive signal that promotes Wnt signaling. The downstream mechanisms for TNF actions include NF-κB and PI3K signaling, which have been shown to cooperate with Wnt to promote β-catenin activation (13, 14, 35). We further propose that TNF regulates ISC and PC populations and contributes to the robust mitogenic crypt responses to mucosal inflammation (as in IBD). Because the effects of TNF signaling deficiencies were most apparent when mice were stimulated with anti-CD3 mAb, we conclude that TNF primarily mediates inflammation-induced IEC Wnt/β-catenin signaling.

These data reveal that TNF directly activates ISC and PC populations during mucosal immune responses and ulcer healing. Comparisons between WT and $Tnf^{-/-}$ IEC responses to T cell activation suggest that TNF induces nuclear p–β-catenin^{552} signaling and proliferation of CBC and PC populations. The role of TNF in mediating ISC and PC responses was seen in WT mice in which exogenous TNF induced β-catenin signaling, BrdU incorporation, and BAT-GAL/TOP-GAL expression in crypt IECs. The induction of BAT-GAL in crypt IECs provides direct evidence for the effect of TNF on Wnt/β-catenin signaling (31). The effect of TNF on ISC/PC populations was further supported in enteroids and colonoid cultures in which TNF induced Wnt/β-catenin target genes (Ascl2, Lgr5, Axin2, CD44 and Lrig). Enhanced TOPFlash activity in NCM460 cells provided further evidence that TNF directly activates epithelial Wnt/β-catenin transcriptional activity. Together, these data suggest that the effects of TNF on Wnt/β-catenin signaling in IECs (ISCs/PCs) support mucosal healing in colitis.

In addition to increasing Wnt/β-catenin signaling and activating mitogenic responses in ISCs/PCs, these data suggest that BM-derived TNF is protective against epithelial apoptosis during inflammation. Previous studies have shown that T cell activation induces epithelial apoptosis in a biphasic manner, differentially affecting villus tip (acute) and crypt apoptosis (>24 h) (24). In mice lacking BM-derived TNF, crypt apoptosis occurred earlier and was more severe than in WT mice. T cell–induced apoptosis has been shown to occur by a variety of mechanisms, including those mediated by TNF, perforin, and Fas/FasL interactions (24, 36). Our data demonstrate that, in the absence of BM-derived TNF, apoptotic responses escalate. In other tissues, enhanced levels of IFN-γ seen in TNF-deficient mice have been proposed to increase programmed cell death (37). Thus, TNF plays an additional regulatory role in the mucosal immune compartment by regulating IFN-γ production and, thereby, curtailing epithelial cell death. The precise nature of the pro- and antiapoptotic impact of TNF on IECs has been observed previously; the investigators proposed that lower TNF levels promote survival signals, whereas higher levels impart proapoptotic effects (38).

A question raised by these studies is how TNF plays dual roles in mucosal inflammation. Clinical data indicate that TNF blockade induces mucosal healing (39), whereas blockade of soluble TNF may make some parameters of colitis worse (6). In WT mice, TNF activates mitogenic ISCs and transit-amplifying responses that aid in ulcer healing. We speculate that the mucosal healing induced by anti-TNF mAb is likely a secondary response to anti-inflammatory depletion of pathogenic effector cells. Anti-TNF induces apoptosis in pathogenic T cells by blocking their interaction with membrane-bound TNF expressing monocytes in a TNFR-dependent manner (39). As demonstrated in $Tnf^{-/-}$ mice, the need for epithelial TNFR signaling becomes more evident in the setting of severe inflammation with high type 1 cytokine levels. In WT→TNFR1/2$^{-/-}$ BMC mice, the loss of IEC TNFR signaling attenuates IEC proliferation and p–β-catenin^{552} levels and worsens mucosal inflammation. However, deficient IEC responses do not cause crypt disruption and loss of mucosal integrity as they do in $Tnf^{-/-}$ mice. We suspect that the explanation for these differences relates to the absence of severe tissue inflammation in TNFR1/2$^{-/-}$ BMC mice. Thus, anti-TNF likely reduces the need for TNF in ISC and PC activation. A concern raised by data in this study is that anti-TNF mAb therapy may reduce ISC/PC activation in patients with persistent mucosal inflammation (as in Fig. 1). Continuation of ineffective TNF blockade in these patients may impair mucosal healing rather than have neutral clinical effects. Interestingly, clinical studies with etanercept, a soluble TNFR:Fc fusion protein, have been uniformly negative (6). Given that etanercept does not induce effector cell apoptosis, we speculate that TNF neutralization in these patients may impair IEC TNF signaling without sufficiently inhibiting mucosal inflammation. Thus, reduced TNF available to IECs may have contributed to the negative clinical outcomes observed.

In summary, these data support the novel idea that TNF promotes mucosal healing in colitis through actions on colonic epithelial stem and progenitor cell populations. Schwitalla et al. (40) suggested that TNF may enhance Wnt/β-catenin activation through NF-κB signaling. In this article, we suggest that this pathway may be active (and helpful) in mucosal healing responses during colitis. Abundant data indicate that TNF is crucial to normal host defenses to enteric pathogens (41). In IBD, the same mechanisms are called into play as the mucosa heals ulcers caused by dysfunctional inflammation. Future studies are needed to determine whether this pathway can be usurped at the epithelial level to aid mucosal repair in patients refractory to standard therapies.

Acknowledgments

We thank L. Li for generously providing p–β-catenin^{552} Ab and D.J.S. for control and anti-TNF murine chimeric mAbs.

Disclosures

T.A.B. is an honorary speaker for Janssen Research and Development and AbbVie Pharmaceuticals. D.J.S. is an employee of Janssen Research and Development. The other authors have no financial conflicts of interest.

References

1. Bradley, J. R. 2008. TNF-mediated inflammatory disease. *J. Pathol.* 214: 149–160.
2. Fujino, S., A. Andoh, S. Bamba, A. Ogawa, K. Hata, Y. Araki, T. Bamba, and Y. Fujiyama. 2003. Increased expression of interleukin 17 in inflammatory bowel disease. *Gut* 52: 65–70.
3. Fuss, I. J., M. Neurath, M. Boirivant, J. S. Klein, C. de la Motte, S. A. Strong, C. Fiocchi, and W. Strober. 1996. Disparate CD4+ lamina propria (LP) lymphokine secretion profiles in inflammatory bowel disease. Crohn's disease LP cells manifest increased secretion of IFN-gamma, whereas ulcerative colitis LP cells manifest increased secretion of IL-5. *J. Immunol.* 157: 1261–1270.
4. Neurath, M. F. 2014. Cytokines in inflammatory bowel disease. *Nat. Rev. Immunol.* 14: 329–342.
5. Rogler, G., and T. Andus. 1998. Cytokines in inflammatory bowel disease. *World J. Surg.* 22: 382–389.
6. Sandborn, W. J., S. B. Hanauer, S. Katz, M. Safdi, D. G. Wolf, R. D. Baerg, W. J. Tremaine, T. Johnson, N. N. Diehl, and A. R. Zinsmeister. 2001. Etanercept for active Crohn's disease: a randomized, double-blind, placebo-controlled trial. *Gastroenterology* 121: 1088–1094.
7. Waetzig, G. H., P. Rosenstiel, A. Arlt, A. Till, K. Bräutigam, H. Schäfer, S. Rose-John, D. Seegert, and S. Schreiber. 2005. Soluble tumor necrosis factor (TNF) receptor-1 induces apoptosis via reverse TNF signaling and autocrine transforming growth factor-beta1. *FASEB J.* 19: 91–93.

8. Marchal Bressenot, A., and L. Peyrin-Biroulet. 2016. Letter: histological assessment of disease activity in ulcerative colitis–the problem of score evaluation and validation; authors' reply. *Aliment. Pharmacol. Ther.* 43: 439.
9. Topol, L., X. Jiang, H. Choi, L. Garrett-Beal, P. J. Carolan, and Y. Yang. 2003. Wnt-5a inhibits the canonical Wnt pathway by promoting GSK-3-independent beta-catenin degradation. *J. Cell Biol.* 162: 899–908.
10. Pinto, D., A. Gregorieff, H. Begthel, and H. Clevers. 2003. Canonical Wnt signals are essential for homeostasis of the intestinal epithelium. *Genes Dev.* 17: 1709–1713.
11. Sato, T., R. G. Vries, H. J. Snippert, M. van de Wetering, N. Barker, D. E. Stange, J. H. van Es, A. Abo, P. Kujala, P. J. Peters, and H. Clevers. 2009. Single Lgr5 stem cells build crypt-villus structures in vitro without a mesenchymal niche. *Nature* 459: 262–265.
12. Lee, G., T. Goretsky, E. Managlia, R. Dirisina, A. P. Singh, J. B. Brown, R. May, G. Y. Yang, J. W. Ragheb, B. M. Evers, et al. 2010. Phosphoinositide 3-kinase signaling mediates beta-catenin activation in intestinal epithelial stem and progenitor cells in colitis. *Gastroenterology* 139: 869–881, 881.e1–9.
13. He, X. C., T. Yin, J. C. Grindley, Q. Tian, T. Sato, W. A. Tao, R. Dirisina, K. S. Porter-Westpfahl, M. Hembree, T. Johnson, et al. 2007. PTEN-deficient intestinal stem cells initiate intestinal polyposis. *Nat. Genet.* 39: 189–198.
14. He, X. C., J. Zhang, W. G. Tong, O. Tawfik, J. Ross, D. H. Scoville, Q. Tian, X. Zeng, X. He, L. M. Wiedemann, et al. 2004. BMP signaling inhibits intestinal stem cell self-renewal through suppression of Wnt-beta-catenin signaling. *Nat. Genet.* 36: 1117–1121.
15. Barker, N., R. A. Ridgway, J. H. van Es, M. van de Wetering, H. Begthel, M. van den Born, E. Danenberg, A. R. Clarke, O. J. Sansom, and H. Clevers. 2009. Crypt stem cells as the cells-of-origin of intestinal cancer. *Nature* 457: 608–611.
16. Miyoshi, H., and T. S. Stappenbeck. 2013. In vitro expansion and genetic modification of gastrointestinal stem cells in spheroid culture. *Nat. Protoc.* 8: 2471–2482.
17. Qiu, W., Y. Hu, T. E. Andersen, A. Jafari, N. Li, W. Chen, and M. Kassem. 2010. Tumor necrosis factor receptor superfamily member 19 (TNFRSF19) regulates differentiation fate of human mesenchymal (stromal) stem cells through canonical Wnt signaling and C/EBP. *J. Biol. Chem.* 285: 14438–14449.
18. Fevr, T., S. Robine, D. Louvard, and J. Huelsken. 2007. Wnt/beta-catenin is essential for intestinal homeostasis and maintenance of intestinal stem cells. *Mol. Cell. Biol.* 27: 7551–7559.
19. van der Flier, L. G., M. E. van Gijn, P. Hatzis, P. Kujala, A. Haegebarth, D. E. Stange, H. Begthel, M. van den Born, V. Guryev, I. Oving, et al. 2009. Transcription factor achaete scute-like 2 controls intestinal stem cell fate. *Cell* 136: 903–912.
20. Flavin, P., A. Redmond, J. McBryan, S. Cocchiglia, P. Tibbitts, P. Fahy-Browne, E. Kay, A. Treumann, K. Perrem, M. McIlroy, et al. 2011. RuvBl2 cooperates with Ets2 to transcriptionally regulate hTERT in colon cancer. *FEBS Lett.* 585: 2537–2544.
21. Powell, A. E., Y. Wang, Y. Li, E. J. Poulin, A. L. Means, M. K. Washington, J. N. Higginbotham, A. Juchheim, N. Prasad, S. E. Levy, et al. 2012. The pan-ErbB negative regulator Lrig1 is an intestinal stem cell marker that functions as a tumor suppressor. *Cell* 149: 146–158.
22. Clayburgh, D. R., T. A. Barrett, Y. Tang, J. B. Meddings, L. J. Van Eldik, D. M. Watterson, L. L. Clarke, R. J. Mrsny, and J. R. Turner. 2005. Epithelial myosin light chain kinase-dependent barrier dysfunction mediates T cell activation-induced diarrhea in vivo. *J. Clin. Invest.* 115: 2702–2715.
23. Tang, Y., D. R. Clayburgh, N. Mittal, T. Goretsky, R. Dirisina, Z. Zhang, M. Kron, D. Ivancic, R. B. Katzman, G. Grimm, et al. 2010. Epithelial NF-kappaB enhances transmucosal fluid movement by altering tight junction protein composition after T cell activation. *Am. J. Pathol.* 176: 158–167.
24. Miura, N., M. Yamamoto, M. Fukutake, N. Ohtake, S. Iizuka, A. Ishige, H. Sasaki, K. Fukuda, T. Yamamoto, and S. Hayakawa. 2005. Anti-CD3 induces bi-phasic apoptosis in murine intestinal epithelial cells: possible involvement of the Fas/Fas ligand system in different T cell compartments. *Int. Immunol.* 17: 513–522.
25. Goretsky, T., R. Dirisina, P. Sinh, N. Mittal, E. Managlia, D. B. Williams, D. Posca, H. Ryu, R. B. Katzman, and T. A. Barrett. 2012. p53 mediates TNF-induced epithelial cell apoptosis in IBD. *Am. J. Pathol.* 181: 1306–1315.
26. Church, D. N., and D. C. Talbot. 2012. Survivin in solid tumors: rationale for development of inhibitors. *Curr. Oncol. Rep.* 14: 120–128.
27. Cohran, V., E. Managlia, E. M. Bradford, T. Goretsky, T. Li, R. B. Katzman, P. Cheresh, J. B. Brown, J. Hawkins, S. X. Liu, et al. 2016. Epithelial PIK3R1 (p85) and TP53 regulate survivin expression during adaptation to ileocecal resection. *Am. J. Pathol.* 186: 1837–1846.
28. Raj, D., T. Liu, G. Samadashwily, F. Li, and D. Grossman. 2008. Survivin repression by p53, Rb and E2F2 in normal human melanocytes. *Carcinogenesis* 29: 194–201.
29. Martini, E., E. Schneider, C. Neufert, M. F. Neurath, and C. Becker. 2016. Survivin is a guardian of the intestinal stem cell niche and its expression is regulated by TGF-β. *Cell Cycle* 15: 2875–2881.
30. Martini, E., N. Wittkopf, C. Günther, M. Leppkes, H. Okada, A. J. Watson, E. Podstawa, I. Backert, K. Amann, M. F. Neurath, and C. Becker. 2016. Loss of survivin in intestinal epithelial progenitor cells leads to mitotic catastrophe and breakdown of gut immune homeostasis. *Cell Reports* 14: 1062–1073.
31. Maretto, S., M. Cordenonsi, S. Dupont, P. Braghetta, V. Broccoli, A. B. Hassan, D. Volpin, G. M. Bressan, and S. Piccolo. 2003. Mapping Wnt/beta-catenin signaling during mouse development and in colorectal tumors. *Proc. Natl. Acad. Sci. USA* 100: 3299–3304.
32. Koch, S., P. Nava, C. Addis, W. Kim, T. L. Denning, L. Li, C. A. Parkos, and A. Nusrat. 2011. The Wnt antagonist Dkk1 regulates intestinal epithelial homeostasis and wound repair. *Gastroenterology* 141: 259–268, 268.e1–8.
33. Nava, P., S. Koch, M. G. Laukoetter, W. Y. Lee, K. Kolegraff, C. T. Capaldo, N. Beeman, C. Addis, K. Gerner-Smidt, I. Neumaier, et al. 2010. Interferon-gamma regulates intestinal epithelial homeostasis through converging beta-catenin signaling pathways. *Immunity* 32: 392–402.
34. Miyoshi, H., R. Ajima, C. T. Luo, T. P. Yamaguchi, and T. S. Stappenbeck. 2012. Wnt5a potentiates TGF-β signaling to promote colonic crypt regeneration after tissue injury. *Science* 338: 108–113.
35. Barrett, T. A. 2012. Developmental biology. Intestinal wound healing requires a Wnt balancing act. *Science* 338: 51–52.
36. Merger, M., J. L. Viney, R. Borojevic, D. Steele-Norwood, P. Zhou, D. A. Clark, R. Riddell, R. Maric, E. R. Podack, and K. Croitoru. 2002. Defining the roles of perforin, Fas/FasL, and tumour necrosis factor alpha in T cell induced mucosal damage in the mouse intestine. *Gut* 51: 155–163.
37. Zganiacz, A., M. Santosuosso, J. Wang, T. Yang, L. Chen, M. Anzulovic, S. Alexander, B. Gicquel, Y. Wan, J. Bramson, et al. 2004. TNF-alpha is a critical negative regulator of type 1 immune activation during intracellular bacterial infection. *J. Clin. Invest.* 113: 401–413.
38. Leppkes, M., M. Roulis, M. F. Neurath, G. Kollias, and C. Becker. 2014. Pleiotropic functions of TNF-α in the regulation of the intestinal epithelial response to inflammation. *Int. Immunol.* 26: 509–515.
39. Atreya, R., M. Zimmer, B. Bartsch, M. J. Waldner, I. Atreya, H. Neumann, K. Hildner, A. Hoffman, R. Kiesslich, A. D. Rink, et al. 2011. Antibodies against tumor necrosis factor (TNF) induce T-cell apoptosis in patients with inflammatory bowel diseases via TNF receptor 2 and intestinal $CD14^+$ macrophages. *Gastroenterology* 141: 2026–2038.
40. Schwitalla, S., A. A. Fingerle, P. Cammareri, T. Nebelsiek, S. I. Göktuna, P. K. Ziegler, O. Canli, J. Heijmans, D. J. Huels, G. Moreaux, et al. 2013. Intestinal tumorigenesis initiated by dedifferentiation and acquisition of stem-cell-like properties. *Cell* 152: 25–38.
41. Beutler, B., and G. E. Grau. 1993. Tumor necrosis factor in the pathogenesis of infectious diseases. *Crit. Care Med.* 21 (10 Suppl): S423–S435.